Engineering Science and Technology, an International Journal 18 (2015) 207–217

HOSTED BY

ELSEVIER

Contents lists available at ScienceDirect

Engineering Science and Technology, an International Journal

journal homepage: http://www.elsevier.com/locate/jestch

Full length article

Analysis of thin film flow over a vertical oscillating belt with a second grade fluid

Taza Gul [a], Saeed Islam [a], Rehan Ali Shah [b], Ilyas Khan [d,*], Sharidan Shafie [c], Muhammad Altaf Khan [a]

[a] Department of Mathematics, Abdul Wali K.U Mardan, Khyber Pakhtunkhwa (KPK) Pakistan
[b] Department of Mathematics, U.E.T Peshawar, Khyber Pakhtunkhwa (KPK) Pakistan
[c] Department of Mathematical Sciences, Faculty of Science, Universiti Teknologi Malaysia, 81310, UTM Johor Bahru, Johor, Malaysia
[d] Department of Basic Sciences, College of Engineering Majmaah University, P.O. Box 66, Majmaah 11952, Saudi Arabia

ARTICLE INFO

Article history:
Received 8 September 2014
Received in revised form
3 November 2014
Accepted 4 November 2014
Available online 20 January 2015

Keywords:
Unsteady flow
Lifting
Drainage
Second grade fluid
ADM
OHAM

ABSTRACT

An analysis is performed to study the unsteady thin film flow of a second grade fluid over a vertical oscillating belt. The governing equation for velocity field with appropriate boundary conditions is solved analytically using Adomian decomposition method (ADM). Expressions for velocity field have been obtained. Optimal asymptotic method (OHAM) has also been used for comparison. The effects of Stocks number, frequency parameter and pressure gradient parameters have been sketched graphically and discussed.

© 2015 Karabuk University. Production and hosting by Elsevier B.V. This is an open access article under the CC BY-NC-ND license (http://creativecommons.org/licenses/by-nc-nd/3.0/).

1. Introduction

The flow of thin fluid has many applications in our daily life. In engineering we see their usage in condensers, distillation units and heat exchangers. In geophysical events we see thin fluid films in the forms of drilling mud, heat pipes and debris flow. In biological science thin fluid films coating the airways in the lungs and thin tear films covering the eye.

On the other hand, non-Newtonian fluids in view of their numerous applications in engineering and industry have been widely studied. For example, few of these applications in industry are found in wire and fiber coating, paper production, transpiration cooling and gaseous diffusion. Considerable efforts have been made to study non-Newtonian fluids through analytical and numerical treatment. Rehan et al. [1] studied unsteady flow of a second grade fluid between a wire and die with one oscillating boundary and other stationary.

The physical importance of thin film has been investigated and discussed by various scientists [2–6]. Amongst them, the thin film flow of a power law model liquid falling down an inclined plate was discussed by Miladinova et al. [7], where they observed that saturation of non-linear interaction occurred in a finite amplitude permanent wave. Alam et al. [8] investigated the thin-film flow of Johnson-Segalman fluids for lifting and drainage problems and observed the effects of various parameters on the lift and drainage velocity profiles. In the literature several mathematical models of non-Newtonian fluids have been proposed. One of the well-known model amongst the non-Newtonian fluids is a subclass of differential type fluids known as second grade fluids which has its constitutive equations based on strong theoretical foundations. Based on this motivation, for the present research we have chosen the second grade fluid as non-Newtonian fluid.

In order to solve the real world problems, different numerical, exact and approximate techniques have been used in mathematics, fluid mechanics and engineering sciences [9–11]. Some of the common methods are HAM and OHAM [12,13]. Application of optimal homotopy asymptotic method for solving non-linear

* Corresponding author.
E-mail address: ilyaskhanqau@yahoo.com (I. Khan).
Peer review under responsibility of Karabuk University.

http://dx.doi.org/10.1016/j.jestch.2014.11.003
2215-0986/© 2015 Karabuk University. Production and hosting by Elsevier B.V. This is an open access article under the CC BY-NC-ND license (http://creativecommons.org/licenses/by-nc-nd/3.0/).

equations arising in heat transfer was investigated by Marinca et al. [14]. In another investigation Marinca et al. [15] have used optimal homotopy asymptotic method for the steady flow of a fourth-grade fluid past a porous plate. Besides that the thin film unsteady flow with variable viscosity has been investigated by Nadeem and Awais [16]. They have analyzed the effect of variable thermo capillarity on the flow and heat transfer. Khajohnsaksumeth et al. [17] studied the effects of slip boundary conditions on the flow of a non-Newtonian fluid through micro channels. They used modified second-grade fluid model where they represented viscosity and the normal stresses in terms of shear rate. The application of their work is focused on blood flow in the cardiovascular system. Taza Gul et al. [18] used ADM and OHAM for the solution of thin film flow of a third grade fluid on a vertical belt with slip boundary conditions. They analyzed the comparison of these two methods.

The main aim of the present work is to study the effects of oscillation into a thin film flow of an unsteady second grade fluid over a vertical belt using ADM and OHAM [19–24].

2. Basic equations

The constitutive equations for an incompressible unsteady flow are

$$\nabla\cdot\mathbf{u} = 0, \tag{1}$$

$$\rho\frac{D\mathbf{u}}{Dt} = \nabla\cdot\mathbf{T} + \rho\mathbf{g}, \tag{2}$$

where ρ is the constant density, $\mathbf{g}$ is used as force per unit mass, $\mathbf{u}$ is the velocity vector, $\mathbf{L} = \nabla\mathbf{u}$, $D/Dt = \partial/\partial t + (\mathbf{u}\cdot\nabla)$ denotes material time derivative and $\mathbf{T}$ is the Cauchy stress tensor which has the following form for a second grade fluid

$$\mathbf{T} = -p\mathbf{I} + \mu\mathbf{A}_1 + \alpha_1\mathbf{A}_2 + \alpha_2\mathbf{A}_1^2. \tag{3}$$

here $-p\mathbf{I}$ denote spherical stress, α_1 and α_2 are the material constants and $\mathbf{A}_1$, $\mathbf{A}_2$ are the kinematical tensors defined as:

$$\mathbf{A}_1 = (\nabla\mathbf{u}) + (\nabla\mathbf{u})^T, \tag{4}$$

$$\mathbf{A}_n = \frac{D\mathbf{A}_{\mathbf{n}-1}}{Dt} + \mathbf{A}_{\mathbf{n}-1}(\nabla\mathbf{u}) + (\nabla\mathbf{u})^T\mathbf{A}_{\mathbf{n}-1}, \quad n > 1. \tag{5}$$

3. Formulation of the lift problem

Consider a wide flat belt moving vertically upward at time $t > 0$, the belt is oscillated and translated with constant speed U through a large bath of second grade liquid. The belt carries with itself a layer of liquid of constant thickness δ. Coordinate system is chosen for analysis in which the x-axis is taken parallel to the surface of the belt and y-axis is perpendicular to the belt. Uniform magnetic field is applied transversely to the belt. Assuming the flow is unsteady and laminar after a small distance above the liquid surface layer.

The velocity field for the present flow is defined as:

$$\mathbf{u} = (0, u(x,t), 0) \tag{6}$$

The associated boundary conditions are:

$$\mathbf{u}(x,t) = U + U\Omega cos\omega t \quad \text{at } x = 0, \quad \frac{\partial\mathbf{u}(x,t)}{\partial x} = 0 \quad \text{at } x = \delta. \tag{7}$$

Here Ω is used as amplitude and ω is used as frequency of the oscillating belt.

Inserting the velocity field from Eq. (6) in continuity Eq. (1) and in momentum Eqs. (2) and (3), the continuity Eq. (1) satisfies identically and Eqs. (2) and (3) are reduced to the following components of stress tensor

$$T_{xx} = -P + (2\alpha_1 + \alpha_2)\left(\frac{\partial u}{\partial x}\right)^2, \tag{8}$$

$$T_{xy} = \mu\frac{\partial u}{\partial x} + \alpha_1\frac{\partial}{\partial t}\left(\frac{\partial u}{\partial x}\right), \tag{9}$$

$$T_{yy} = -P + \alpha_2\left(\frac{\partial u}{\partial x}\right)^2, \tag{10}$$

$$T_{zz} = -P, \tag{11}$$

$$T_{xz} = T_{yz} = 0. \tag{12}$$

Making use of Eqs. (8)–(12) into Eq. (3), we get

$$\rho\frac{\partial u}{\partial t} = -\frac{\partial p}{\partial y} + \mu\frac{\partial^2 u}{\partial x^2} + \alpha_1\frac{\partial}{\partial t}\left(\frac{\partial^2 u}{\partial x^2}\right) - \rho g. \tag{13}$$

Introducing the following non-dimensional variables

$$\tilde{u} = \frac{u}{U}, \ \tilde{x} = \frac{x}{\delta}, \ \tilde{t} = \frac{\mu t}{\rho\,\delta^2}, \ \tilde{\omega} = \frac{\omega\,\delta^2\rho}{\mu}, \ \lambda = \frac{\delta^2\partial p}{\mu\,U\partial y}, \quad S_t = \frac{\delta^2\rho g}{\mu\,U}, \ \alpha = \frac{\alpha_1}{\rho\,\delta^2}, \tag{14}$$

where ω is the frequency parameter, λ is non-dimensional pressure gradient parameter, α is the non-Newtonian parameter, t is time parameter and S_t is the Stock's number.

Introducing Eq. (14) into Eq. (13) and dropping out the bar notations, we obtain

$$\frac{\partial u}{\partial t} = -\lambda + \frac{\partial^2 u}{\partial x^2} + \alpha\frac{\partial}{\partial t}\left(\frac{\partial^2 u}{\partial x^2}\right) - S_t. \tag{15}$$

The corresponding boundary conditions (7) are reduced to

$$u_n(0,t) = 1 + \Omega\cos\omega t \ , \ and \ \frac{du_n(1,t)}{dx} = 0, \quad n = 0, \tag{16}$$

$$u_n(0,t) = 0, \quad \frac{du_n(1,t)}{dx} = 0, \quad n \geq 1. \tag{17}$$

4. Analysis of Adomain decomposition method

The Adomian decomposition method (ADM) is used to decompose the unknown function $u(x,t)$ into a sum of an infinite number of components defined by the decomposition series.

$$u(x,t) = \sum_{n=0}^{\infty} u_n(x,t), \tag{18}$$

The decomposition method is used to find the components. $u_0(x,t)$,$u_1(x,t)$,$u_2(x,t)$… separately. The determination of these components can be obtained through simple integrals. To give a clear overview of (ADM), we consider the partial differential equation in an operator form as

$$L_t u(x,t) + L_x u(x,t) + Ru(x,t) + Nu(x,t) = g(x,t), \tag{19}$$

$$L_x u(x,t) = g(x,t) - L_t u(x,t) - Ru(x,t) - Nu(x,t), \tag{20}$$

where $L_x = \partial^2/\partial x^2$ and $L_t = \partial/\partial t$ are linear operators in the partial differential equation and are easily invertible, $g(x, t)$ is a source term, $Ru(x, t)$ is a remaining linear term and $Nu(x, t)$ is non-linear analytical term expandable in the Adomian polynomials A_n.

After applying the inverse operator L_x^{-1} to both sides of Eq. (20), we write

$$L_x^{-1}L_x u(x,t) = L_x^{-1}g(x,t) - L_x^{-1}L_t u(x,t) - L_x^{-1}Ru(x,t) - L_x^{-1}Nu(x,t), \tag{21}$$

$$u(x,t) = f(x,t) - L_x^{-1}L_t u(x,t) - L_x^{-1}Ru(x,t) - L_x^{-1}Nu(x,t). \tag{22}$$

Here the function $f(x, t)$ represents the terms arising from $L^{-1}g(x, t)$, after using the given conditions. $L_x^{-1} = \iint(.)dxdx$ is used as inverse operator for the second order partial differential equation.

Adomian decomposition method defines the series solution $u(x, t)$ as

$$u(x,t) = \sum_{k=0}^{\infty} u_n(x,t), \tag{23}$$

$$\sum_{n=0}^{\infty} u_n(x,t) = f(x,t) - L_x^{-1}L_t \sum_{n=0}^{\infty} u_n(x,t) - L_x^{-1}R\sum_{n=0}^{\infty} u_n(x,t) - L_x^{-1}N\sum_{n=0}^{\infty} u_n(x,t). \tag{24}$$

The non-linear term is expanded in Adomian polynomials as

$$N\sum_{n=0}^{\infty} u_n(x,t) = \sum_{n=0}^{\infty} A_n, \tag{25}$$

where the components $u_0(x, t)$, $u_1(x, t)$, $u_2(x, t)$…… are periodically derived as,

$$\begin{aligned} u_0(x,t) + u_1(x,t) + u_2(x,t)\ldots = {} & f(x,t) - L_x^{-1}L_t(u_0(x,t) + u_1(x,t) \\ & + u_2(x,t)\ldots) - L_x^{-1}R(u_0(x,t) \\ & + u_1(x,t) + u_2(x,t)\ldots) \\ & - L_x^{-1}(A_0 + A_1 + A_2\ldots). \end{aligned} \tag{26}$$

To determine the components of the series $u_0(x, t) + u_1(x, t) + u_2(x, t)$…… it is important to note that ADM suggests that the zeroth component $u_0(x, t)$ is usually defined by the function $f(x, t)$ described above.

The formal recursive relation is defined as:

$$\begin{aligned} u_0(x,t) &= f(x,t), \\ u_1(x,t) &= -L_x^{-1}L_t[u_0(x,t)] - L_x^{-1}R[u_0(x,t)] - L_x^{-1}[A_0], \\ u_2(x,t) &= -L_x^{-1}L_t[u_1(x,t)] - L_x^{-1}R[u_1(x,t)] - L_x^{-1}[A_1], \\ u_3(x,t) &= -L_x^{-1}L_t[u_2(x,t)] - L_x^{-1}R[u_2(x,t)] - L_x^{-1}[A_2], \quad \text{and so on.} \end{aligned} \tag{27}$$

5. Optimal homotopy asymptotic method

For the analysis of OHAM we consider the boundary value problem as consider in [14]:

$$\tilde{L}(\tilde{u}(x)) + \tilde{N}(\tilde{u}(x)) + \tilde{G}(x) = 0, \quad \tilde{B}\left(\tilde{u}, \frac{\partial \tilde{u}}{\partial x}\right) = 0, \tag{28}$$

where $\tilde{L}$ a linear operator in the differential equation is, $\tilde{N}$ is a non-linear term, $x \in R$ is an independent variable, $\tilde{B}$ is a boundary operator and $\tilde{G}$ is a source term. According to [14] we construct a set of equation for OHAM.

$$\begin{aligned} [1-p]\left[\tilde{L}\tilde{\varphi}(x,p) + \tilde{G}(x)\right] &= H(p)\left[\tilde{L}\tilde{\varphi}(x,p) + \tilde{G}(x) + \tilde{N}\tilde{\varphi}(x,p)\right], \\ \tilde{B}\left(\tilde{\varphi}(x,p), \frac{\partial \tilde{\varphi}(x,p)}{\partial x}\right) &= 0, \end{aligned} \tag{29}$$

$p \in [0, 1]$ is an embedding parameter, $H(p)$, is a non-zero auxiliary function for $p \neq 0$ and $H(0) = 0$. $\tilde{\varphi}(x, p)$ is an unknown function. Obviously, when $p = 0$ and $p = 1$, it holds that:

$$\tilde{\varphi}(x,0) = \tilde{u}_0(x), \quad \tilde{\varphi}(x,1) = \tilde{u}(x), \tag{30}$$

when p varies from 0 to 1 then $\tilde{\varphi}(x, p)$ also varies from $\tilde{u}_0(x)$ to $\tilde{u}(x)$. Where the zero component solution $\tilde{u}_0(x)$ is obtained from Eq. (29) when $p = 0$,

$$\tilde{L}(\tilde{u}_0(x)) + \tilde{G}(x) = 0, \quad \tilde{B}\left(\tilde{u}_0(x), \frac{\partial \tilde{u}_0(x)}{\partial x}\right) = 0, \tag{31}$$

Auxiliary function $H(p)$ is choosing as

$$H(p) = pc_1 + p^2c_2 + \ldots, \tag{32}$$

c_1, c_2 are auxiliary constants.

Marinca [14] uses a special procedure to expand $\tilde{\varphi}(x, p)$ with respect to p by using Taylor series.

$$\tilde{\varphi}(x,p,c_i) = \tilde{u}_0(x) + \sum_{k\geq 1} \tilde{u}_k(x,c_i)p^k, \quad i = 1, 2, \ldots. \tag{33}$$

Inserting Eq. (33) into Eq. (29), collecting the same powers of p, and equating each coefficient of p, the zero order problem is given in equation (31) and the first and second order are given in Eqs. (34) and (35).

$$\tilde{L}(\tilde{u}_1(x)) + \tilde{G}(x) = c_1\tilde{N}_0(\tilde{u}_0(x)), \quad \tilde{B}\left(\tilde{u}_1(x), \frac{\partial \tilde{u}_1(x)}{\partial x}\right) = 0, \tag{34}$$

$$\begin{aligned} \tilde{L}(\tilde{u}_2(x)) - \tilde{L}(\tilde{u}_1(x)) &= c_2\tilde{N}_0(\tilde{u}_0(x)) \\ &\quad + c_1\left[\tilde{L}(\tilde{u}_1(x)) + \tilde{N}_1(\tilde{u}_0(x), \tilde{u}_1(x))\right], \\ \tilde{B}\left(\tilde{u}_2(x), \frac{\partial \tilde{u}_2(x)}{\partial x}\right) &= 0. \end{aligned} \tag{35}$$

The general governing equations for $u_k(x)$ are given by

$$\tilde{L}(\tilde{u}_k(x)) - \tilde{L}(\tilde{u}_{k-1}(x)) = c_k\tilde{N}_0(\tilde{u}_0(x)) + \sum_{i=1}^{k-1} c_i\left[\tilde{L}(\tilde{u}_{k-i}(x)) + \tilde{N}_{k-1}(\tilde{u}_0(x), \tilde{u}_1(x)..\tilde{u}_{k-i}(x))\right], \quad k = 2, 3, \ldots, \ \tilde{B}\left(\tilde{u}_k(x), \ \frac{\partial \tilde{u}_k(x)}{\partial x}\right) = 0, \tag{36}$$

here $\tilde{N}_m(\tilde{u}_0(x), \tilde{u}_1(x)..\tilde{u}_{m-1}(x))$ is the coefficient of p^m, in the expansion of $\tilde{N}\tilde{\varphi}(x, p)$.

$$\tilde{N}(\tilde{\varphi}(x, p, c_i)) = \tilde{N}_0(\tilde{u}_0(x)) + \sum_{m=1}^{\infty} \tilde{N}_m(\tilde{u}_0(x), \tilde{u}_1(x)..\tilde{u}_m(x))p^m. \tag{37}$$

The convergence of the Series in Eq. (33) depend upon the auxiliary constants c_1, c_2,… If it converges at $p = 1$, then the mth order approximation $\tilde{u}$ is

$$\tilde{u}(x, c_1, c_2 \ldots c_m) = \tilde{u}_0(x) + \sum_{i=1}^{m} \tilde{u}_i(x, c_1, c_2 \ldots c_i). \tag{38}$$

Inserting Eq. (38) into Eq. (28), the residual is obtained as:

$$\tilde{R}(x, c_i) = \tilde{L}(\tilde{u}(x, c_i)) + \tilde{G}(x) + \tilde{N}(\tilde{u}(x, c_i)), \quad i = 1, 2 \ldots m \tag{39}$$

Numerous methods like Ritz Method, Method of Least Squares, Galerkin's Method and Collocation Method are used to find the optimal values of c_i, i = 1,2,3,4…. We apply the Method of Least Squares in our problem as given below:

$$J(c_1, c_2, \ldots c_n) = \int_a^b \tilde{R}^2(x, c_1, c_2, \ldots c_m)dx, \tag{40}$$

where a and b are the constant values taking from domain of the problem.

Auxiliary constants (c_1, c_2,…c_n) can be identified from:

$$\frac{\partial J}{\partial c_1} = \frac{\partial J}{\partial c_2} = \ldots = 0. \tag{41}$$

Finally, from these auxiliary constants, the approximate solution is well-determined.

6. Solution of lifting problem

6.1. ADM solution

The inverse operator $L_x^{-1} = \iint(.)dx$ is applied on the second order differential Eq. (15) and according to the standard form of ADM from Eq. (22):

$$u(x, t) = f(x) + L_x^{-1}(L_t u) - \alpha L_x^{-1}[L_t(L_x u)], \tag{42}$$

with $L_t = \partial/\partial t, \ L_x = \partial^2/\partial x^2$,

$$\text{so that } u(x, t) = f(x) + L_x^{-1}\left(\frac{\partial}{\partial t}u\right) - \alpha L_x^{-1}\left[\frac{\partial}{\partial t}\left(\frac{\partial^2 u}{\partial x^2}\right)\right]. \tag{43}$$

Summation is used for the series solutions of Eq. (43):

$$\sum_{n=0}^{\infty} u_n(x, t) = f(x) + L_x^{-1}\left(\frac{\partial}{\partial t}\sum_{n=0}^{\infty} u_n(x, t)\right) - \alpha L_x^{-1}\left[\frac{\partial}{\partial t}\left(\frac{\partial^2}{\partial x^2}\sum_{n=0}^{\infty} u_n(x, t)\right)\right]. \tag{44}$$

The series solution of Eq. (44) is derived as:

$$u_0(x, t) + u_1(x, t) + u_2(x, t) + \ldots = f(x) + L_x^{-1}\left(\frac{\partial}{\partial t}(u_0(x, t) + u_1(x, t) + u_2(x, t) + \ldots)\right) - \alpha L_x^{-1}\left[\frac{\partial}{\partial t}\left(\frac{\partial^2}{\partial x^2}(u_0(x, t) + u_1(x, t) + u_2(x, t) + \ldots)\right)\right]. \tag{45}$$

The velocity components are obtained by comparing both sides of Eq. (45).

Components of the lift problem up to second order are:

$$u_0(x, t) = f(x) = L_x^{-1}\left(\frac{\partial^2 u_0}{\partial x^2} - S_t - p\right), \tag{46}$$

$$u_1(x, t) = L_x^{-1}\frac{\partial u_0}{\partial t} - \alpha L_x^{-1}\left[\frac{\partial}{\partial t}\left(\frac{\partial^2 u_0}{\partial x^2}\right)\right], \tag{47}$$

$$u_2(x, t) = L_x^{-1}\frac{\partial u_1}{\partial t} - \alpha L_x^{-1}\left[\frac{\partial}{\partial t}\left(\frac{\partial^2 u_1}{\partial x^2}\right)\right]. \tag{48}$$

Making use of boundary conditions from Eqs. (16) and (17) into Eqs. (46)–(48), the zero, first and second components solutions are obtained as:

$$u_0(x, t) = \frac{1}{2}(-1 + x)(-2 + x\lambda - 2\Omega\mathrm{Cos}[t\omega] + xS_t), \tag{49}$$

$$u_1(x, t) = \frac{1}{6}\left(-2x\omega\mathrm{Sin}[t\omega] + 3x^2\omega\mathrm{Sin}[t\omega] - x^3\omega\mathrm{Sin}[t\omega]\right), \tag{50}$$

$$u_2(x, t) = \frac{1}{360}\left(-8x\omega^2\mathrm{Cos}[t\omega] + 20x^3\omega^2\mathrm{Cos}[t\omega] - 15x^4\omega^2\mathrm{Cos}[t\omega] + 3x^5\omega^2\mathrm{Cos}[t\omega] - 120x\alpha\omega^2\mathrm{Cos}[t\omega] + 180x^2\alpha\omega^2\mathrm{Cos}[t\omega] - 60x^3\alpha\omega^2\mathrm{Cos}[t\omega]\right). \tag{51}$$

The series solution up to the second component is given as:

$$u(x, t) = u_0(x, t) + u_1(x, t) + u_2(x, t). \tag{52}$$

Inserting components solutions from Eqs. (49)–(51), in the series solution (52), we have:

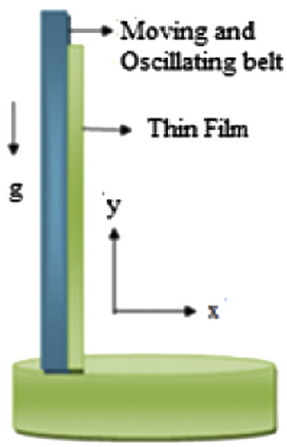

Fig. 1. Geometry of Lift problem.

$$
\begin{aligned}
u(x,t) =& \frac{1}{360}\Big(-8x\omega^2\mathrm{Cos}[t\omega] + 20x^3\omega^2\mathrm{Cos}[t\omega] \\
&- 15x^4\omega^2\mathrm{Cos}[t\omega] + 3x^5\omega^2\mathrm{Cos}[t\omega] - 120x\alpha\omega^2\mathrm{Cos}[t\omega] \\
&+ 180x^2\alpha\omega^2\mathrm{Cos}[t\omega] - 60x^3\alpha\omega^2\mathrm{Cos}[t\omega]\Big) \\
&+ \frac{1}{6}\Big(-2x\omega\mathrm{Sin}[t\omega] + 3x^2\omega\mathrm{Sin}[t\omega] - x^3\omega\mathrm{Sin}[t\omega]\Big) \\
&+ \frac{1}{2}(-1+x)(-2+x\lambda - 2\Omega\mathrm{Cos}[t\omega] - xS_t).
\end{aligned} \tag{53}
$$

6.2. OHAM solution

We formulate a homotopy for Eq. (15) from the standard form of OHAM into Eq. (29). According to above discussion the zero, first and second component problems are:

$$
p^0: \quad \lambda + S_t - \frac{\partial^2 u_0}{\partial x^2} = 0. \tag{54}
$$

$$
\begin{aligned}
p^1: \quad & -\lambda - \lambda c_1 - S_t - c_1 S_t - c_1\frac{\partial u_0}{\partial t} + \frac{\partial^2 u_0}{\partial x^2} + c_1\frac{\partial^2 u_0}{\partial x^2} \\
& + \alpha c_1\frac{\partial}{\partial t}\left(\frac{\partial^2 u_0}{\partial x^2}\right) - \frac{\partial^2 u_1}{\partial x^2} = 0,
\end{aligned} \tag{55}
$$

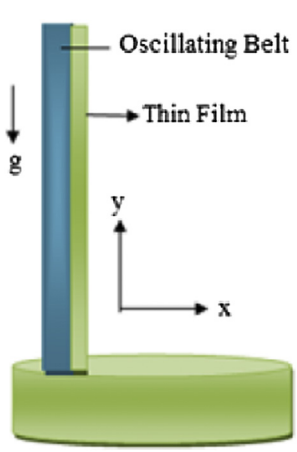

Fig. 2. Geometry of Drainage problem.

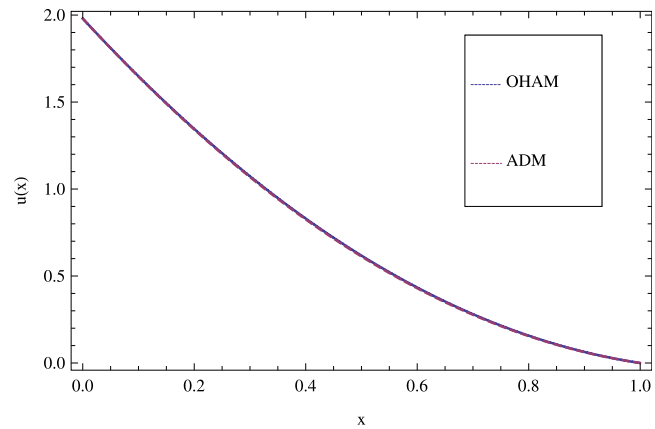

Fig. 3. Comparison of ADM and OHAM methods for lift velocity profile $\omega = 0.2$, $\alpha = 0.02$, $U = 1$, $S_t = 1$, $\lambda = 2$, $\Omega = 1$.

$$
\begin{aligned}
p^2: \quad & -\lambda c_2 - c_2 S_t - c_2\frac{\partial u_0}{\partial t} - c_1\frac{\partial u_1}{\partial t} + c_2\frac{\partial^2 u_0}{\partial x^2} + \alpha c_2\frac{\partial}{\partial t}\left(\frac{\partial^2 u_0}{\partial x^2}\right) \\
& + \frac{\partial^2 u_1}{\partial x^2} + c_1\frac{\partial^2 u_1}{\partial x^2} + \alpha c_1\frac{\partial}{\partial t}\left(\frac{\partial^2 u_1}{\partial x^2}\right) - \frac{\partial^2 u_2}{\partial x^2} = 0.
\end{aligned} \tag{56}
$$

Solving Eqs. (54)–(56) by using the corresponding boundary conditions given in Eqs. (16) and (17) are

$$
u_0(x,t) = \frac{1}{2}(-1+x)(-2+x\lambda - 2\Omega\mathrm{Cos}[t\omega] + xS_t), \tag{57}
$$

$$
u_1(x,t,c_1) = \frac{1}{6}\Big(-2x\omega\mathrm{Sin}[t\omega]c_1 + 3x^2\omega\mathrm{Sin}[t\omega]c_1 - x^3\omega\mathrm{Sin}[t\omega]c_1\Big), \tag{58}
$$

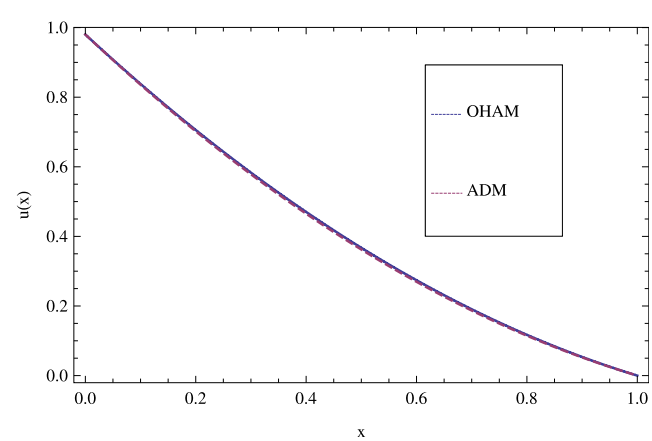

Fig. 4. Comparison of ADM and OHAM methods for drainage velocity profile $c_1 = -1.001669$, $c_2 = -0.000189$.

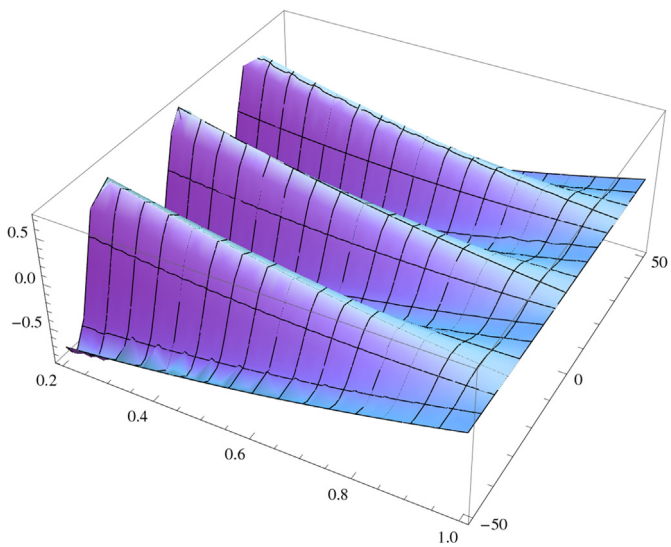

Fig. 5. Influence of different time level on lift velocity profile.

$$
\begin{aligned}
u_2(x,t,c_2) = \frac{1}{360}\Big(&-120x\omega\mathrm{Sin}[t\omega]c_1 + 180x^2\omega\mathrm{Sin}[t\omega]c_1 \\
&- 60x^3\omega\mathrm{Sin}[t\omega]c_1 - 8x\omega^2\mathrm{Cos}[t\omega]c_1^2 \\
&+ 20x^3\omega^2\mathrm{Cos}[t\omega]c_1^2 - 15x^4\omega^2\mathrm{Cos}[t\omega]c_1^2 \\
&+ 3x^5\omega^2\mathrm{Cos}[t\omega]c_1^2 - 120x\alpha\omega^2\mathrm{Cos}[t\omega]c_1^2 \\
&+ 180x^2\alpha\omega^2\mathrm{Cos}[t\omega]c_1^2 - 60x^3\alpha\omega^2\mathrm{Cos}[t\omega]c_1^2 \\
&- 120x\omega\mathrm{Sin}[t\omega]c_1^2 + 180x^2\omega\mathrm{Sin}[t\omega]c_1^2 \\
&- 60x^3\omega\mathrm{Sin}[t\omega]c_1^2 - 120x\omega\mathrm{Sin}[t\omega]c_2 \\
&+ 180x^2\omega\mathrm{Sin}[t\omega]c_2 - 60x^3\omega\mathrm{Sin}[t\omega]c_2\Big).
\end{aligned} \tag{59}
$$

The series solution of velocity profile is:

$$\tilde{u}(x,t,c_i) = u_0(x,t) + u_1(x,t,c_1) + u_2(x,t,c_2). \tag{60}$$

The arbitrary constants C_i, $i = 1,2$ are find out by using the residual:

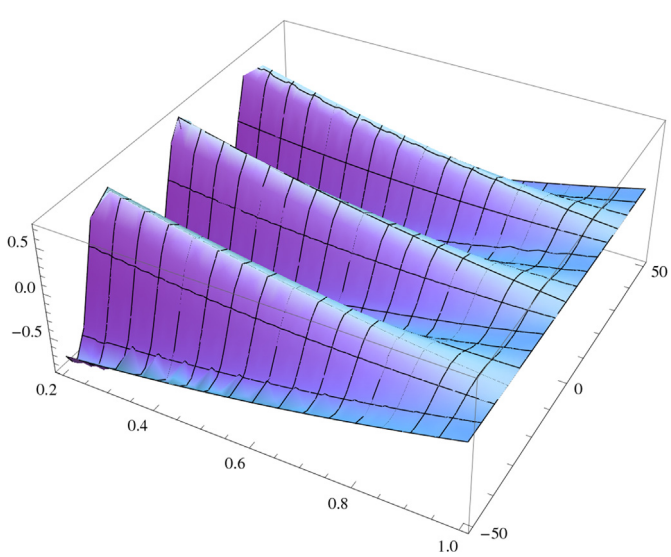

Fig. 6. Influence of different time level on drainage velocity.

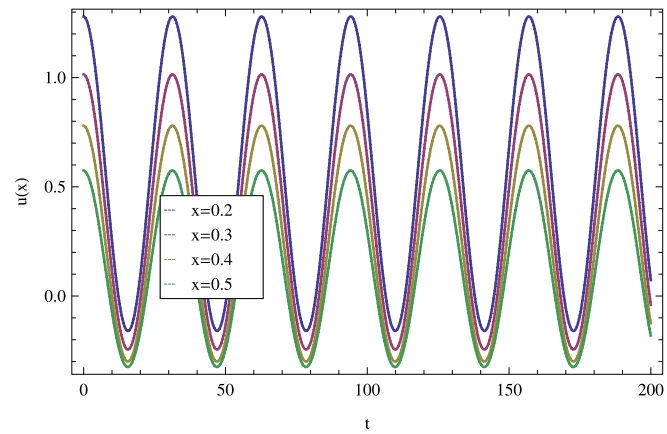

Fig. 7. Lift velocity distribution of fluid when $\omega = 0.2$, $\alpha = 0.02$, $S_t = 1$, $\lambda = 2$, $\xi = 0.9$.

$$R = \tilde{L}(\tilde{u}(x,t,c_i)) + \tilde{N}(\tilde{u}(x,t,c_i)) + \tilde{G}(\tilde{u}(x,t,c_i)). \tag{61}$$

According to Eqs. (40) and (41), the arbitrary constants for velocity components $u_0(x, t)$, $u_1(x, t, c_1)$ and $u_2(x, t, c_2)$ are:

$$
\begin{aligned}
c_1 &= -1.0016691463222276, \\
c_2 &= -0.0001895412688948106.
\end{aligned} \tag{62}
$$

Inserting the auxiliary constants from Eq. (62) in the series solution (60), we obtained the velocity profile as:

$$
\begin{aligned}
u(x,t) = \frac{1}{360}\Big(&-8.02673x\omega^2\mathrm{Cos}[t\omega] + 20.06682x^3\omega^2\mathrm{Cos}[t\omega] \\
&- 15.05012x^4\omega^2\mathrm{Cos}[t\omega] + 3.01003x^5\omega^2\mathrm{Cos}[t\omega] \\
&- 120.40093x\alpha\omega^2\mathrm{Cos}[t\omega] + 180.60139x^2\alpha\omega^2\mathrm{Cos}[t\omega] \\
&- 60.20046x^3\alpha\omega^2\mathrm{Cos}[t\omega] - 0.17788x\omega\mathrm{Sin}[t\omega] \\
&+ 0.26683x^2\omega\mathrm{Sin}[t\omega] - 0.08894x^3\omega\mathrm{Sin}[t\omega]\Big) \\
&+ \frac{1}{6}\Big(2.00334x\omega\mathrm{Sin}[t\omega] - 3.00501x^2\omega\mathrm{Sin}[t\omega] \\
&+ 1.00167x^3\omega\mathrm{Sin}[t\omega]\Big) + \frac{1}{2}(-1+x)(-2+x\lambda \\
&- 2\Omega\mathrm{Cos}[t\omega] - xS_t).
\end{aligned} \tag{63}
$$

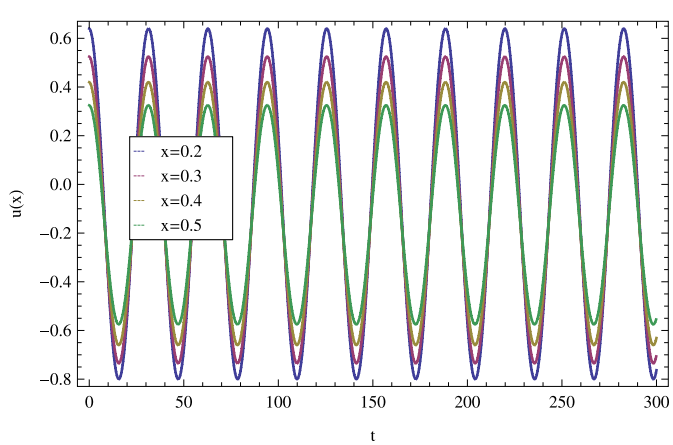

Fig. 8. Drainage velocity distribution of fluid when $\omega = 0.2$, $\alpha = 0.02$, $S_t = 1$, $\lambda = 2$, $\xi = 0.9$.

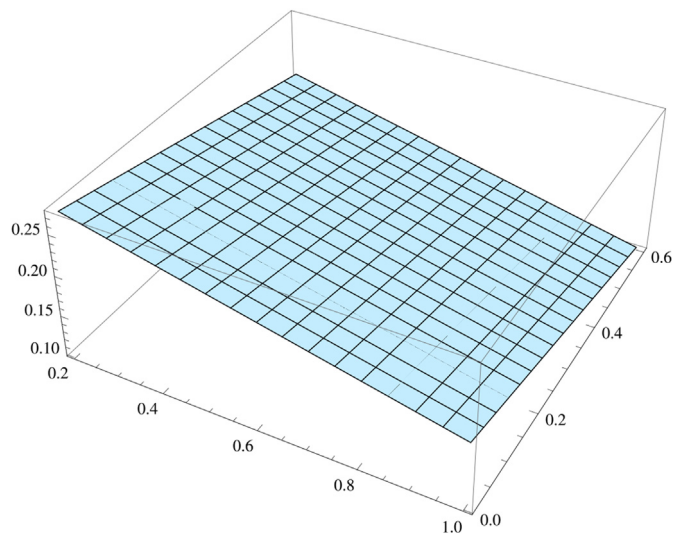

Fig. 9. Combine effect of the Stock number and pressure gradient parameter on the lift velocity when $\omega = 0.2$, $\alpha = 0.02$, $t = 10$, $x = 0.5$, $\xi = 0.9$.

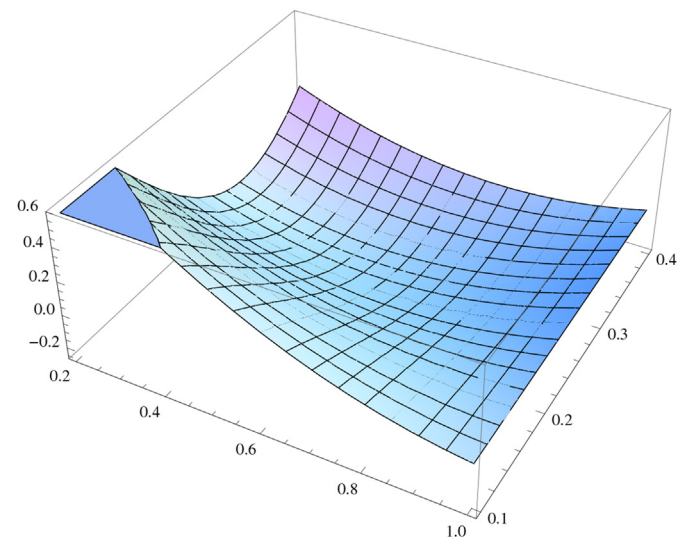

Fig. 11. Effect of frequency parameter on the lift velocity when $\omega = 0.2$, $\alpha = 0.02$, $S_n = 0.4$, $\lambda = 2$, $t = 10$, $\xi = 0.9$.

7. Formulation of drainage problem

The geometry and assumptions of the problem are same as in previous problem. We consider a film of non-Newtonian liquid drains down the vertical belt. The belt is only oscillating and the fluid drain down the belt due to gravity. The gravity in this case is opposite to the previous case. The coordinate system is selected same as in previous case. Assuming the flow is unsteady and laminar, consider fluid shear forces keep the gravity balanced and the film thickness remains constant.

Boundary conditions for drainage problem:

$$\mathbf{u}(x,t) = \Omega cos\omega t \quad \text{at } x = 0, \qquad \frac{\partial \mathbf{u}(x,t)}{\partial x} = 0 \text{ at } x = \delta. \tag{64}$$

Using non-dimensional variables from Eq. (14), the governing Eq. (13) and boundary conditions (64) of drainage problem are reduced to:

$$\frac{\partial u}{\partial t} = -p + \frac{\partial^2 u}{\partial x^2} + \alpha \frac{\partial}{\partial t}\left(\frac{\partial^2 u}{\partial x^2}\right) + S_t, \tag{65}$$

$$u_n(o,t) = \Omega \cos \omega t, \ \ and \frac{du_n(1,t)}{dx} = 0, \ \ n = 0. \tag{66}$$

8. Solution of drainage problem

8.1. ADM solution

The model for drainage problem is same as for the left problem. The only difference is that due to the draining of thin film the Stock number is positively mentioned in Eq. (65).

Components of the lift problem up to second order are:

$$u_0(x,t) = f(x) = L_x^{-1}\left(\frac{\partial^2 u_0}{\partial x^2} + S_t - \lambda\right). \tag{67}$$

Making use of boundary conditions from Eq. (59) in Eq. (60) the zero component solution is obtained as:

$$u_0(x,t) = \frac{1}{2}(-1+x)(x\lambda - 2\Omega \mathrm{Cos}[t\omega] - xS_t). \tag{68}$$

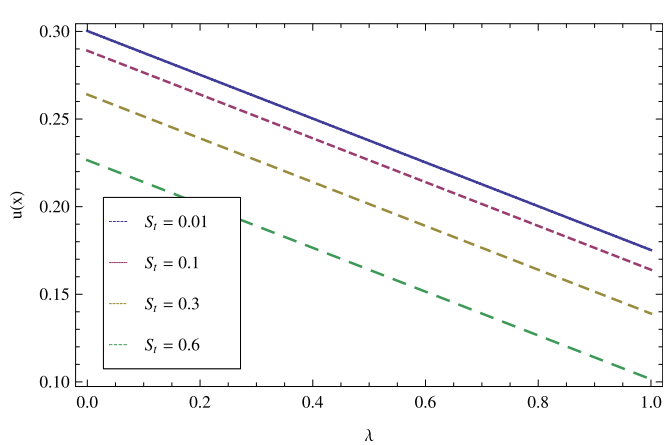

Fig. 10. Combine effect of the Stock number and pressure gradient parameter on the lift velocity when $\omega = 0.2$, $\alpha = 0.02$, $t = 10$, $x = 0.5$, $\xi = 0.9$.

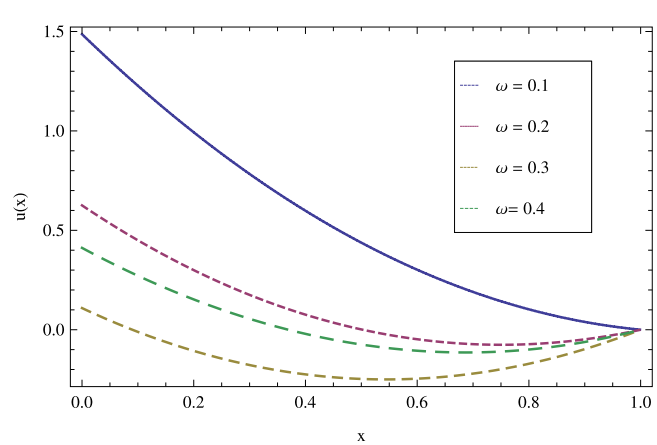

Fig. 12. Effect of frequency parameter on the lift velocity when $\omega = 0.2$, $\alpha = 0.02$, $S_n = 0.4$, $\lambda = 2$, $t = 10$, $\xi = 0.9$.

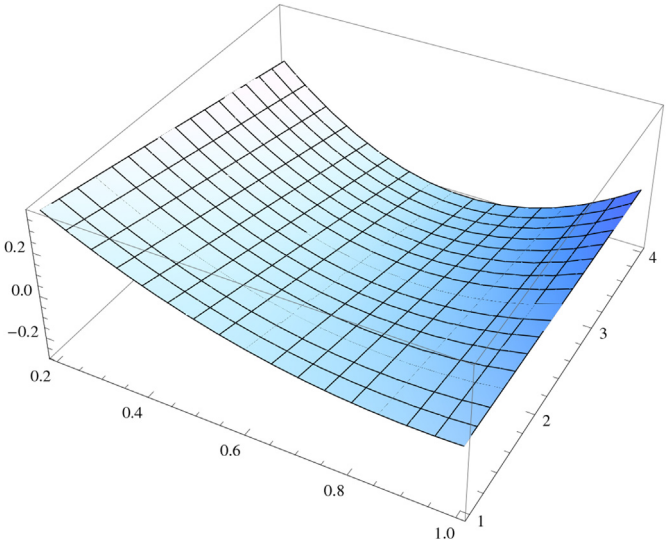

Fig. 13. The effect of non-dimensional λ, on lift velocity when $\omega = 0.2$, $\alpha = 0.02$, $S_t = 0.4$, $t = 10$, $\xi = 0.9$.

The first and second components solution mentioned in Eqs. (50) and (51) are same due to the same boundary conditions of Eq. (17).

The series solution up to the second component is as:

$$u(x,t) = u_0(x,t) + u_1(x,t) + u_2(x,t). \tag{69}$$

Inserting components solutions from Eq. (68) and from Eqs. (60) and (61), in the series solution (68) we have:

$$\begin{aligned} u(x,t) = \frac{1}{360}\Big(&- 8x\omega^2\mathrm{Cos}[t\omega] + 20x^3\omega^2\mathrm{Cos}[t\omega] - 15x^4\omega^2\mathrm{Cos}[t\omega] \\ &+ 3x^5\omega^2\mathrm{Cos}[t\omega] - 120x\alpha\omega^2\mathrm{Cos}[t\omega] + 180x^2\alpha\omega^2\mathrm{Cos}[t\omega] \\ &- 60x^3\alpha\omega^2\mathrm{Cos}[t\omega]\Big) + \frac{1}{6}\Big(- 2x\omega\mathrm{Sin}[t\omega] + 3x^2\omega\mathrm{Sin}[t\omega] \\ &- x^3\omega\mathrm{Sin}[t\omega]\Big) + \frac{1}{2}(-1+x)(x\lambda - 2\Omega\mathrm{Cos}[t\omega] - xS_t). \end{aligned} \tag{70}$$

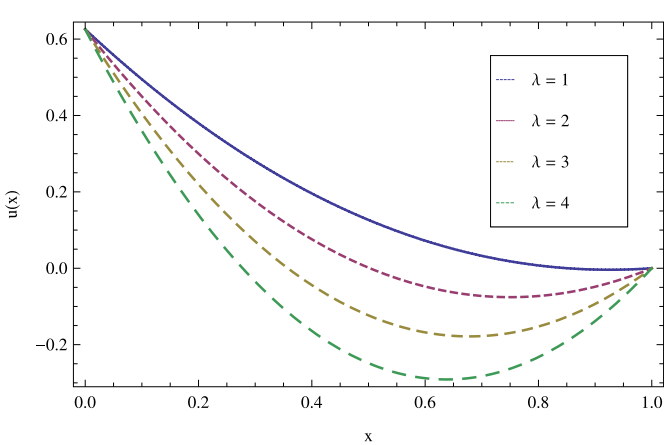

Fig. 14. The effect of non-dimensional λ, on lift velocity when $\omega = 0.2$, $\alpha = 0.02$, $S_t = 0.4$, $t = 10$, $\xi = 0.9$.

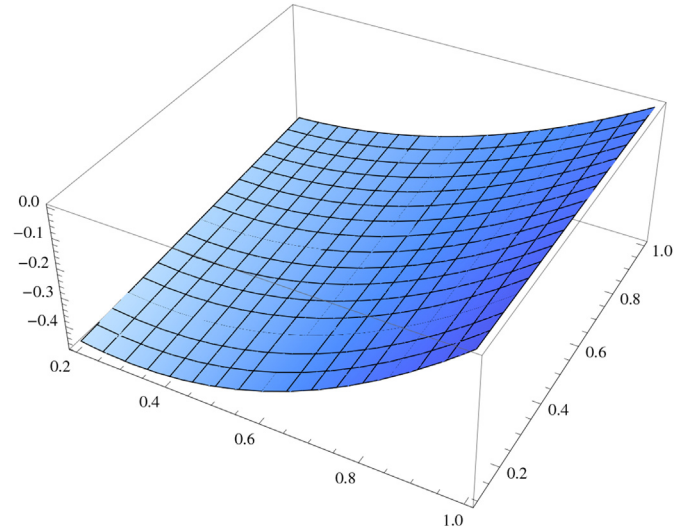

Fig. 15. Effect of S_t, on drain velocity profile when $\omega = 0.2$, $\alpha = 0.02$, $\lambda = 2$, $t = 10$, $\xi = 0.9$.

8.2. OHAM solution

From the standard form of OHAM in Eq. (29), we construct a homotopy for Eq. (65). According to above discussion the zero, first and second component problems are:

$$p^0 : \lambda - S_t - \frac{\partial^2 u_0}{\partial x^2} = 0, \tag{71}$$

$$\begin{aligned} p^1 : &- \lambda - \lambda c_1 + S_t + c_1 S_t - c_1\frac{\partial u_0}{\partial t} + \frac{\partial^2 u_0}{\partial x^2} + c_1\frac{\partial^2 u_0}{\partial x^2} \\ &+ \alpha c_1\frac{\partial}{\partial t}\left(\frac{\partial^2 u_0}{\partial x^2}\right) - \frac{\partial^2 u_1}{\partial x^2} = 0, \end{aligned} \tag{72}$$

$$\begin{aligned} p^2 : \quad &- \lambda c_2 + c_2 S_t - c_2\frac{\partial u_0}{\partial t} - c_1\frac{\partial u_1}{\partial t} + c_2\frac{\partial^2 u_0}{\partial x^2} + \alpha c_2\frac{\partial}{\partial t}\left(\frac{\partial^2 u_0}{\partial x^2}\right) \\ &+ \frac{\partial^2 u_1}{\partial x^2} + c_1\frac{\partial^2 u_1}{\partial x^2} + \alpha c_1\frac{\partial}{\partial t}\left(\frac{\partial^2 u_1}{\partial x^2}\right) - \frac{\partial^2 u_2}{\partial x^2} = 0. \end{aligned} \tag{73}$$

Solving Eq. (71) by using the corresponding boundary

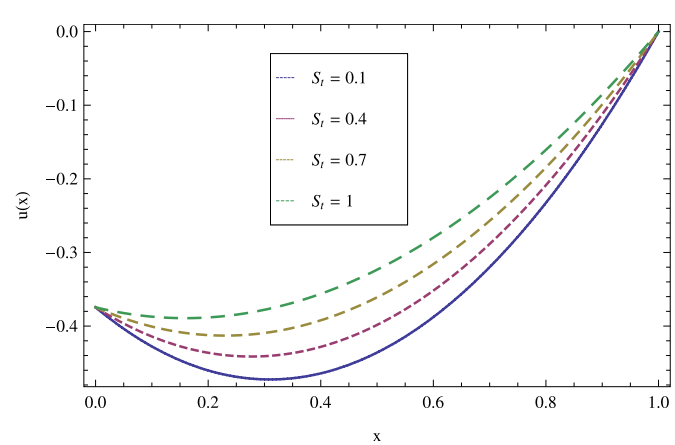

Fig. 16. Effect of S_t, on drain velocity profile when $\omega = 0.2$, $\alpha = 0.02$, $\lambda = 2$, $t = 10$, $\xi = 0.9$.

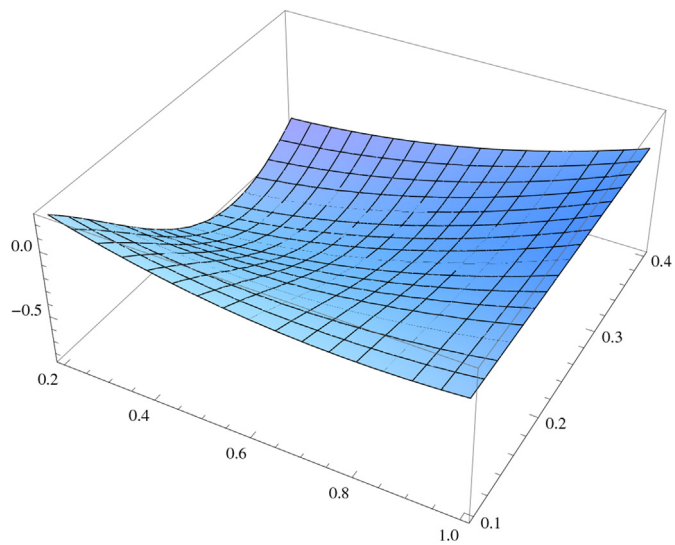

Fig. 17. Effect of frequency ω, on drainage velocity when $\alpha = 0.02$, $S_t = 0.4$, $\lambda = 2$, $t = 10$, $\xi = 0.9$.

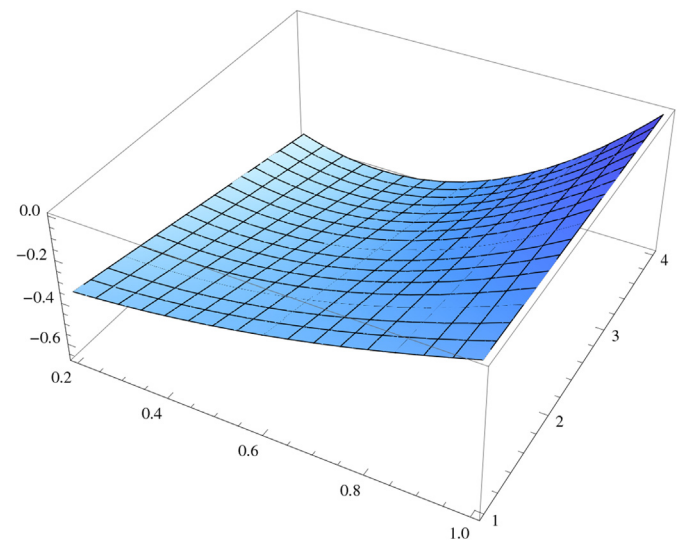

Fig. 19. The effect of bulk modulus on drain velocity when $\omega = 0.2$, $\alpha = 0.02$, $t = 10$, $\xi = 0.9$, $S_t = 0.4$.

conditions given in Eq. (66). The zero component solution obtained as:

$$u_0(x,t) = \frac{1}{2}(-1+x)(xp - 2\Omega \mathrm{Cos}[t\omega] - xS_t). \tag{74}$$

The first and second components solution mentioned in Eqs. (58) and (59) are same due to the same boundary conditions of Eq. (17), and the series solutions of velocity profile is:

$$\tilde{u}(x,t,c_i) = u_0(x,t) + u_1(x,t) + u_2(x,t). \tag{75}$$

Arbitrary constants C_i, $i = 1, 2$ are find out by using the same method mentioned in Eq. (55) whereas the arbitrary constants for velocity components $u_0(x,t)$, $u_1(x,t)$ and $u_2(x,t)$ are same as given in Eq. (62). Inserting the auxiliary constants in the series solution (75), we obtained the velocity profile as:

$$\begin{aligned} u(x,t) =& \frac{1}{360}\Big(-8.02673x\omega^2 \,\mathrm{Cos}[t\omega] + 20.06682x^3\omega^2 \,\mathrm{Cos}[t\omega] \\ & - 15.05012x^4\omega^2 \,\mathrm{Cos}[t\omega] + 3.01003x^5\omega^2 \,\mathrm{Cos}[t\omega] \\ & - 120.40093x\alpha\omega^2 \,\mathrm{Cos}[t\omega] + 180.60139x^2\alpha\omega^2 \,\mathrm{Cos}[t\omega] \\ & - 60.20046x^3\alpha\omega^2 \,\mathrm{Cos}[t\omega] - 0.17788x\omega \,\mathrm{Sin}[t\omega] \\ & + 0.26683x^2\omega \,\mathrm{Sin}[t\omega] - 0.08894x^3\omega \mathrm{Sin}[t\omega]\Big) \\ & + \frac{1}{6}\Big(2.00334x\omega \,\mathrm{Sin}[t\omega] - 3.00501x^2\omega \,\mathrm{Sin}[t\omega] \\ & + 1.00167x^3\omega \,\mathrm{Sin}[t\omega]\Big) + \frac{1}{2}(-1+x) \\ & \times (x\lambda - 2\Omega \,\mathrm{Cos}[t\omega] - xS_t) \end{aligned} \tag{76}$$

9. Results and discussion

In this article we present and interpret several results for the thin film unsteady flow of a second grade fluid over a vertical belt.

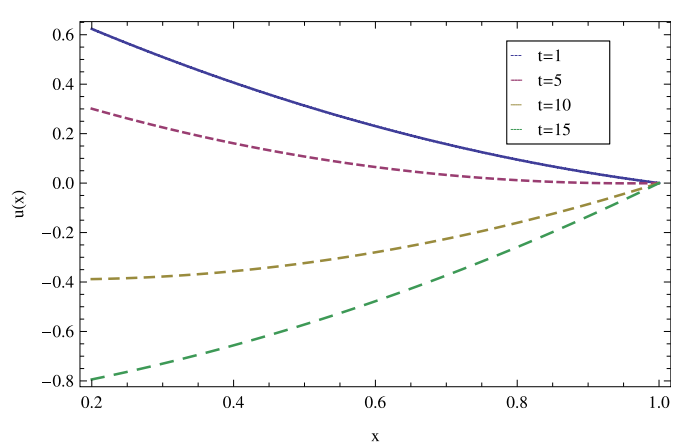

Fig. 18. Effect of frequency ω, on drainage velocity when $\alpha = 0.02$, $S_t = 0.4$, $\lambda = 2$, $t = 10$, $\xi = 0.9$.

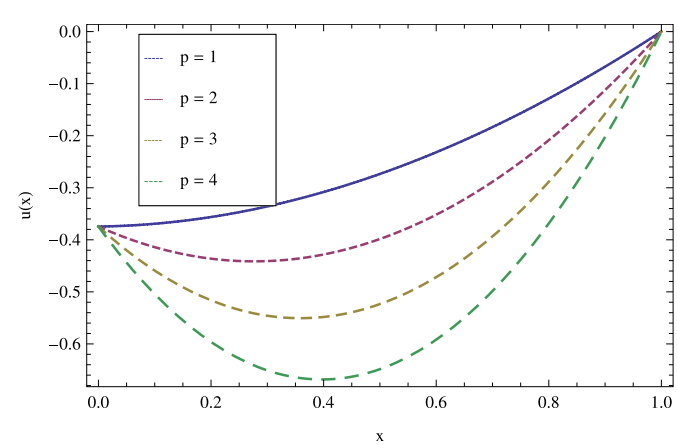

Fig. 20. The effect of bulk modulus on drain velocity when $\omega = 0.2$, $\alpha = 0.02$, $t = 10$, $\xi = 0.9$, $S_t = 0.4$.

Table 1
Comparison of OHAM & ADM for lift velocity when $\omega = 0.2$, $\alpha = 0.02$, $S_t = 0.5$, $\lambda = 2$, $t = 0.01$, $\Omega = 1$.

x	OHAM	ADM	Absolute error
0.0	2	2	0
0.1	1.6874	1.68738	2.24×10^{-5}
0.2	1.39982	1.39978	3.77×10^{-5}
0.3	1.13725	1.13721	4.67×10^{-5}
0.4	0.89972	0.89967	5.01×10^{-5}
0.5	0.68722	0.68716	4.89×10^{-5}
0.6	0.49973	0.49969	4.38×10^{-5}
0.7	0.33727	0.33724	3.35×10^{-5}
0.8	0.19984	0.19982	2.50×10^{-5}
0.9	0.08742	0.08741	1.29×10^{-5}
1.0	1.8131×10^{-19}	1.5419×10^{-19}	2.710×10^{-20}

Table 4
Comparison of OHAM and ADM for drain velocity when $\omega = 0.2$, $\alpha = 0.02$, $S_t = 0.5$, $\lambda = 2$, $t = 0.01$, $\Omega = 1$.

x	OHAM	ADM	Absolute error
0.0	0.999998	0.999998	0
0.1	0.8324	0.832377	2.24×10^{-5}
0.2	0.6798	0.67978	3.77×10^{-5}
0.3	0.5423	0.54220	4.67×10^{-5}
0.4	0.4197	0.41967	5.01×10^{-5}
0.5	0.3122	0.31216	4.89×10^{-5}
0.6	0.2197	0.21968	4.38×10^{-5}
0.7	0.1423	0.14224	3.55×10^{-5}
0.8	0.0798	0.07982	2.50×10^{-5}
0.9	0.0324	0.03241	1.29×10^{-5}
1.0	1.813×10^{-19}	1.541×10^{-19}	2.71×10^{-20}

Figs. 1 and 2 show the geometry of lift and drainage velocity profiles. The effects of non-dimensional physical parameter such as Stock number S_t, frequency parameter ω, pressure gradient parameter λ and non-Newtonian parameter α in lifting and drainage problems are discussed in Figs. 3–20. A comparison of the ADM and OHAM solutions are shown in Figs. 3–6 for various values of physical parameters and are found in excellent agreement. The numerical comparison of ADM and OHAM at different time levels are derived in Tables 1–6 for both lift and drainage velocity profiles respectively. It is observed from these tables that absolute error between ADM and OHAM decreases with decrease in time level, while it increases with increase in time level. As the flow of fluid film is subjected to the oscillation as well as translation of the belt, so the velocity of the fluid film will be high at the surface of the belt comparatively to the residual domain and will decrease gradually for the fluid film away from the surface of the belt. These conclusions are observed from Tables 7 and 8 and Figs. 7 and 8. The velocity of belt decreases with increasing Stock number in lift velocity profile. So increase in S_t and λ decreases velocity of fluid film observed in Figs. 9 and 10. In Figs. 11, 12 and 17,18 both consecutively for lift and drainage velocity profiles, increase in non-dimensional frequency ω change the direction of fluid flow frequently and steadily converges to a point on the surface of the fluid. If the belt velocity increases with oscillation, then the centripetal force decreases which results in decrease in the velocity of fluid. The effect of pressure gradient parameter λ on lift and drainage velocity distribution is consecutively derived in Figs. 13 and 14 and in 19,20. Increase in λ decreases the velocity of fluid because it is inversely proportional to velocity of the belt. Figs. 15 and 16 show the effect of Stock number on drainage velocity profile. During oscillation of the belt, Stock number is proportional to the drainage velocity of fluid. Therefore, increase in Stock number increases the velocity of fluid.

Table 2
Comparison of OHAM & ADM for lift velocity when $\omega = 0.2$, $\alpha = 0.02$, $S_t = 0.5$, $\lambda = 2$, $t = 0.03$, $\Omega = 1$.

x	OHAM	ADM	Absolute error
0.0	1.99998	1.99998	0
0.1	1.68741	1.68734	2.24×10^{-5}
0.2	1.39984	1.39973	3.77×10^{-5}
0.3	1.13729	1.13715	4.67×10^{-5}
0.4	0.89976	0.89961	5.01×10^{-5}
0.5	0.68726	0.68711	4.89×10^{-5}
0.6	0.49977	0.49964	4.38×10^{-5}
0.7	0.33731	0.33719	3.35×10^{-5}
0.8	0.19986	0.19978	2.50×10^{-5}
0.9	0.08743	0.08738	1.29×10^{-5}
1.0	4.168×10^{-19}	1.5419×10^{-20}	4.987×10^{-19}

Table5
Comparison of OHAM and ADM for drain velocity when $\omega = 0.2$, $\alpha = 0.02$, $S_t = 0.5$, $\lambda = 2$, $t = 0.03$, $\Omega = 1$.

x	OHAM	ADM	Absolute error
0.0	0.9999982	0.9999982	0
0.1	0.832408	0.83234	2.24×10^{-5}
0.2	0.679842	0.67973	3.77×10^{-5}
0.3	0.54229	0.54215	4.67×10^{-5}
0.4	0.41976	0.41961	5.01×10^{-5}
0.5	0.31225	0.31211	4.89×10^{-5}
0.6	0.21977	0.21964	4.38×10^{-5}
0.7	0.14231	0.14219	3.55×10^{-5}
0.8	0.07986	0.07978	2.50×10^{-5}
0.9	0.03243	0.03238	1.29×10^{-5}
1.0	4.168×10^{-19}	-8.19×10^{-20}	4.98×10^{-19}

Table3
Comparison of OHAM and ADM for lift velocity when $\omega = 0.2$, $\alpha = 0.02$, $S_t = 0.5$, $\lambda = 2$, $t = 1$, $\Omega = 1$.

x	OHAM	ADM	Absolute error
0.0	1.98007	1.98007	0
0.1	1.67058	1.66832	2.26×10^{-3}
0.2	1.38576	1.38195	3.81×10^{-3}
0.3	1.12565	1.12092	4.72×10^{-3}
0.4	0.89028	0.88519	5.08×10^{-3}
0.5	0.679712	0.674745	4.96×10^{-3}
0.6	0.49397	0.48952	4.44×10^{-3}
0.7	0.33309	0.32947	3.61×10^{-3}
0.8	0.19712	0.19457	2.54×10^{-3}
0.9	0.08607	0.08476	1.31×10^{-3}
1.0	1.927×10^{-18}	1.311×10^{-18}	6.167×10^{-19}

Table 6
Comparison of OHAM and ADM for drainage velocity when $\omega = 0.2$, $\alpha = 0.02$, $S_t = 0.5$, $\lambda = 2$, $t = 1$, $\Omega = 1$.

x	OHAM	ADM	Absolute error
0.0	0.980067	0.980067	0
0.1	0.81558	0.81332	2.26×10^{-3}
0.2	0.66576	0.66195	3.81×10^{-3}
0.3	0.53065	0.52592	4.72×10^{-3}
0.4	0.41028	0.40519	5.08×10^{-3}
0.5	0.304712	0.29975	4.96×10^{-3}
0.6	0.21397	0.20952	4.44×10^{-3}
0.7	0.13809	0.13447	3.61×10^{-3}
0.8	0.07712	0.07457	2.54×10^{-3}
0.9	0.03107	0.02976	1.31×10^{-3}
1.0	1.927×10^{-18}	1.311×10^{-18}	6.167×10^{-19}

Table 7
Lift velocity at various domain points at different time level when $\omega = 0.2$, $\alpha = 0.02$, $S_n = 1$, $\lambda = 2$, $\xi = 0.9$.

t	$x = 0.2$	$x = 0.3$	$x = 0.4$	$x = 0.5$
0	1.2798	1.01473	0.77969	0.57469
1	1.26354	0.999816	0.766395	0.563242
2	1.21924	0.960388	0.732109	0.534324
3	1.14866	0.898022	0.678203	0.489087
4	1.0546	0.815203	0.606828	0.429335
5	0.940831	0.715233	0.520828	0.35745
6	0.811877	0.602097	0.423633	0.276298
7	0.672882	0.480307	0.319117	0.189114
8	0.529386	0.354717	0.211447	0.0993746
9	0.387111	0.230335	0.104915	0.0106565
10	0.251729	0.112118	0.003768	−0.0735031

Table 8
Shows drainage velocity distribution of thin film layer at various domain points at different time level.

t	$x = 0.2$	$x = 0.3$	$x = 0.4$	$x = 0.5$
0	0.639799	0.524733	0.419696	0.32469
1	0.623544	0.509816	0.406395	0.313242
2	0.57924	0.470388	0.372109	0.284324
3	0.508655	0.408022	0.318203	0.239087
4	0.414602	0.325203	0.246828	0.179335
5	0.300831	0.225233	0.160828	0.10745
6	0.171877	0.112097	0.063633	0.026298
7	0.0328819	−0.009693	−0.040883	−0.060886
8	−0.110614	−0.135283	−0.148553	−0.150625
9	−0.252889	−0.259665	−0.255085	−0.239344
10	−0.388271	−0.37882	−0.356232	−0.323503

10. Conclusion

In this article, we have modeled the thin film flow of unsteady second grade fluid over a vertical belt. The belt is oscillating and translating for lift velocity distribution while belt is only oscillating for drainage velocity distribution. The governing problems have been solved analytically by ADM and OHAM. The comparison of (ADM) and (OHAM) has been derived graphically and numerically. Expression for velocity field has been derived and sketched. The effects of various embedded flow parameters have been discussed.

Acknowledgments

The authors would like to acknowledge the financial support of Majmaah University Saudi Arabia, the Ministry of Education Malaysia (MOE) and the Research Management Centre-UTM through vote numbers 06H67 and 4F255 for this research. The corresponding author is also grateful to Majmaah University Saudi Arabia for the financial support through research project.

References

[1] R.A. Shah, S. Islam, A.M. Siddiqui, T. Haroon, OHAM solution of unsteady second grade fluid in wire coating analysis, J. KSIAM 15 (2011) 201–222.
[2] C. Fetecau, C. Fetecau, Starting solutions for the motion of a second grade fluid due to longitudinal and torsional oscillations of a circular cylinder, Int. J. Eng. Sci. 44 (2006) 788–796.
[3] C. Fetecau, C. Fetecau, Starting solutions for some unsteady unidirectional flows of a second grade fluid, Int. J. Eng. Sci. 43 (2005) 781–789.
[4] S. Nadeem, N. Faraz, Thin film flow of a second grade fluid over a stretching/shrinking sheet with variable temperature-dependent viscosity, Chin. Phy. Lett. 27 (2010) 034704.
[5] M. Qasim, I. Khan, S. Shafie, Heat transfer and mass diffusion in nanofluids with convective boundary conditions, Math. Prob. Eng. (2013).
[6] S. Haq, I. Khan, F. Ali, S. Shafie, Radiation and magnetohydrodynamics effects on unsteady free convection flow in a porous medium, Math. Prob. Eng (2013).
[7] S. Miladinova, G. Lebon, E. Toshev, Thin film flow of a power law liquid falling down an inclined plate, J. Non-Newtonian Fluid Mech. 122 (2004) 69–70.
[8] M.K. Alam, M.T. Rahim, T. Haroon, S. Islam, A.M. Siddiqui, Solution of steady thin film flow of Johnson–Segalman fluid on a vertical moving belt for lifting and drainage problems using Adomian decomposition method, Appl. Math. Comput. 218 (2012) 10413–10428.
[9] I. Khan, F. Ali, S. Sharidan, Stokes' second problem for magnetohydrodynamics flow in a burgers' fluid: the cases $\gamma = \lambda^2/4$ and $\gamma > \lambda^2/4$, PLoS One 8 (5) (2013) e61531, http://dx.doi.org/10.1371/journal.pone.0061531.
[10] M. Qasim, I. Khan, S. Sharidan, Heat Transfer in a micropolar fluid over a stretching sheet with newtonian heating, PLoS One 8 (4) (2013) e59393, http://dx.doi.org/10.1371/journal.pone.0059393.
[11] W.A. Khan, I. Pop, Boundary layer flow past a stretching, surface in a porous medium saturated by a nanofluid: Brinkman–Forchheimer model, PLoS One 7 (10) (2012). ArticleID, e47031.
[12] A.M. Siddiqui, R. Mahmood, Q.K. Ghori, Homotopy perturbation method for thin film flow of a third grade fluid down an inclined plane, Chaos Soln. Fract. 35 (1) (2008) 140–147.
[13] S.J. Liao, Beyond Perturbation: Introduction to Homotopy Analysis Method, Chapman & Hall/CRC Press, Boca Raton, 2003.
[14] V. Marinca, N. Herisanu, I. Nemes, Optimal homotopy asymptotic method with application to thin film flow, Cent. Eur. J. Phys. 6 (3) (2008) 648–653.
[15] V. Marinca, N. Herisanu, Application of optimal homotopy asymptotic method for solving non-linear equations arising in heat transfer, Int. Commun. Heat Mass Transfer 35 (2008) 710–715.
[16] S. Nadeem, M. Awais, Thin film flow of an unsteady shrinking sheet through porous medium with variable viscosity, Phy. Lett. A 372 (2008) 4965–4972.
[17] N. Khajohnsaksumeth, B. Wiwatanapataphee, Y.H. Wu, The effect of boundary slip on the transient pulsatile flow of a modified second-grade fluid, Abstr. Appl. Anal. (2013).
[18] T. Gul, R.A. Shah, S. Islam, M. Arif, MHD thin film flows of a third grade fluid on a vertical belt with slip boundary conditions, J. Appl. Math. (2013).
[19] G. Adomian, Solving Frontier Problems of Physics: The Decomposition Method, Kluwer Academic Publishers, 1994.
[20] G. Adomian, A review of the decomposition method and some recent results for non-linear equations, Math. Comput. Model. 13 (1992) 287–299.
[21] A.M. Wazwaz, Adomian decomposition method for a reliable treatment of the Bratu-type equations, Appl. Math. Comput. 166 (2005) 652–663.
[22] A.M. Wazwaz, Adomian decomposition method for a reliable treatment of the Emden-Fowler equation, Appl. Math. Comput. 161 (2005) 543–560.
[23] Y. Cherruault, Convergence of Adomian's method, Kybernotes 18 (20) (1990) 31–38.
[24] Y. Cherruault, G. Adomian, Decomposition methods: a new proof of convergence, Math. Comput. Model. 18 (1993) 103–106.